

Long Range Surface Plasmons for Observation of Biomolecular Binding Events at Metallic Surfaces

Jakub Dostálek · Amal Kasry · Wolfgang Knoll

Received: 19 March 2007 / Accepted: 6 July 2007
© Springer Science + Business Media, LLC 2007

Abstract A long range surface plasmon (LRSP) is an electromagnetic wave propagating along a thin metal film with an order of magnitude lower damping than conventional surface plasmon (SP) waves. Thus, the excitation of LRSP is associated with a narrower resonance and it provides larger enhancement of intensity of the electromagnetic field. In surface plasmon resonance (SPR) biosensors, these features allow a more precise observation of the binding of biomolecules in the proximity to the metal surface by using the (label-free) measurement of refractive index (RI) variations and by SP-enhanced fluorescence spectroscopy. In this contribution, we investigate LRSPs excited on a layer structure consisting of a fluoropolymer buffer layer, a thin gold film, and an aqueous sample. By implementing such structure in an SPR sensor, we achieved a 2.4- and 4.4-fold improvement of the resolution in the label-free and fluorescence-based detection, respectively, of the binding of biomolecules in the close proximity to the surface. Moreover, we demonstrate that the sensor resolution can be improved by a factor of 14 and 12 for the label-free and fluorescence-based detection, respectively, if the

biomolecular binding events occur within the whole evanescent field of LRSP.

Keywords Surface plasmon resonance · Long range surface plasmon · Biosensor · Fluorescence spectroscopy · Optical sensor

Introduction

Surface plasmon resonance (SPR) is an optical phenomenon associated with the resonant excitation of surface plasmons (SPs)-coupled oscillations of the electromagnetic field and the electron density at an interface between a metal and a dielectric [1]. Up to now, SPs have been employed in biosensors based on the label-free and fluorescence-based observations of biomolecular binding events, and they were applied for the detection and interaction analysis of various analytes. In label-free SPR biosensors [2], the binding of target biomolecules to their partners anchored on the metal surface is observed through the binding-induced change in the refractive index (RI). Biosensors utilizing SP-enhanced fluorescence spectroscopy [3] measure light emission of dye-labeled target molecules captured at the metal surface. These devices take advantage of the SP-increased intensity of the electromagnetic field exciting fluorescent dyes.

Long range surface plasmons (LRSPs) are electromagnetic modes formed by the coupling of surface plasmons (SPs) propagating along opposite interfaces of thin metal films sandwiched between two dielectrics with similar refractive indices [4]. LRSPs have a symmetric profile of the magnetic intensity field across the metal layer and exhibit an order of magnitude lower damping compared to conventional SPs [5]. Since the early 1990s, LRSPs have

J. Dostálek (✉) · A. Kasry · W. Knoll
Department of Materials Science,
Max Planck Institute for Polymer Research,
Ackermannweg 10,
55128 Mainz, Germany
e-mail: dostalek@mpip-mainz.mpg.de

Present address:

A. Kasry
Center for Cell Analysis and Modeling (CCAM),
UConn Health Center,
263 Farmington Avenue,
Farmington, CT 06030, USA

attracted attention for the design of high-resolution SPR sensors [6]. Up to now, LRSP-based sensors were mostly applied for measurements of the RI changes in bulk media [7]. Currently, an ultrahigh RI resolution (smallest detectable RI change) of 2.5×10^{-8} refractive index units (RIU) was achieved [8], which is an order of magnitude lower than that typically provided by conventional SPR sensors. However, much less attention was devoted to the implementation of LRSP-based sensors for the detection of RI variations at the sensor surface because of the capture of biomolecules. Until now, LRSP-based sensor with almost the same resolution as that of conventional SPR was reported [9] for such measurements. Only recently, the application of LRSPs for fluorescence spectroscopy as a promising approach to enhance the field intensity of the electromagnetic field exciting the dye-labeled analyte molecules was reported [10].

In this work, we present a detailed study of a multilayer structure supporting LRSPs for the observation of biomolecular binding events on its surface based on two different approaches, i.e., by label-free measurement of RI variations and by fluorescence spectroscopy. The investigated structure consists of a glass substrate with a fluoropolymer buffer layer, a thin gold film, and an aqueous sample on its top. We optimized the structure for label-free and fluorescence-based detection of biomolecular binding events in close proximity of the gold surface and within the whole evanescent field of the LRSP. Achieved improvement in the resolution of the LRSP-based sensor with respect to that of a conventional SPR sensor is compared with theoretical predictions.

Materials and methods

Preparation of layer structures supporting LRSPs

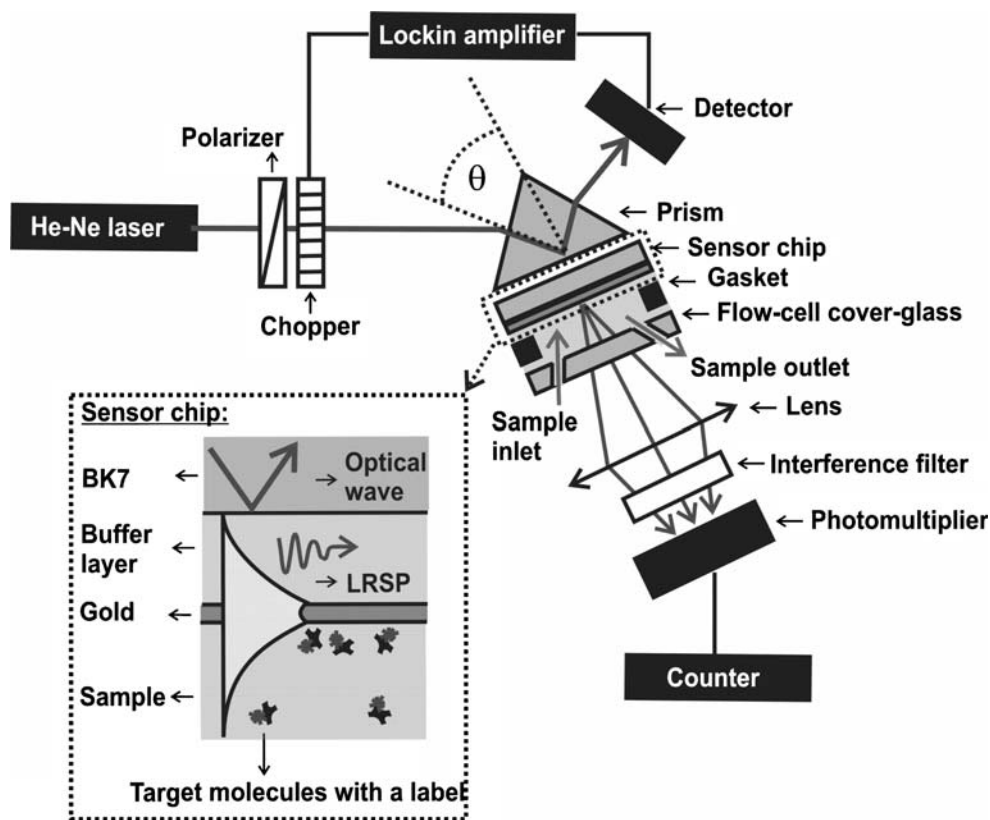
In described experiments, we used a layer structure supporting LRSPs that consisted of a BK7 glass substrate, a fluoropolymer buffer layer, and a thin gold film. We used two commercially available fluoropolymers: Cytop (CTL-809M, ASAHI, Japan; dissolved in the solvent CT-180) and Teflon AF (Teflon AF1600, DuPont, USA; dissolved in the solvent FC-40). At the wavelength of $\lambda=633$ nm, Cytop and Teflon AF exhibit a refractive index, which is slightly above ($n_{\text{Cytop}}=1.340$) and below ($n_{\text{AF}}=1.308$) that of water ($n_{\text{water}}=1.333$), respectively. These fluoropolymers were spincoated on cleaned BK7 substrate with the rotation speed (typically 1,000–4,000 rpm) adjusted such that layers with desired thickness (typically 600–1,000 nm) were produced according to experimentally measured curves. To improve the adhesion of Teflon AF to the BK7

substrate, before its deposition, the BK7 substrate was immersed in 2% solution of perfluorodecyltrichlorosilane (ABCR, Germany) dissolved in toluene for 2 h. Both Teflon AF and Cytop layers were dried at room temperature for 1 h followed by 1 h baking at 160 °C. On the top of the a low-refractive index buffer layer, a thin gold film was deposited by means of thermal evaporation (Edwards FL400, Boc Edwards, U.K.). The deposition of gold (99.99%, Edelmetall, Germany) was performed at room temperature in vacuum better than 5×10^{-6} bar. The thickness of the fluoropolymer buffer layers was measured using a surface profiler (KLA-Tencor P-10). The thickness of the gold films was determined using calibrated quartz crystal. The surface roughness of the deposited thin gold films was observed by an atomic force microscope (Dimensions 3100, Veeco Instruments, USA) operated in the tapping mode.

Optical setup for coupling to LRSPs

For the excitation of LRSPs, we used an optical setup utilizing the angular spectroscopy of SPs and the total internal reflection method (ATR) in the Kretschmann configuration (see Fig. 1). Briefly, a monochromatic light beam from He–Ne laser (PL610P, Polytec, Germany, power 2 mW, wavelength $\lambda=632.8$ nm) was linearly polarized using a polarizer, passed through a chopper (Princeton Applied Research, USA) and was coupled to a BK7 prism. Onto the prism base, a BK7 glass slide with a layer structure supporting LRSPs (fluoropolymer layer and gold film with a thickness of 15–30 nm) or conventional SPs (gold film with a thickness of 50 nm) was optically matched using immersion oil (Cargile, USA). The intensity of the light beam reflected at the prism base was measured using a photodetector and a lock-in amplifier (Model 5210, Princeton Applied Research, USA). The angle of incidence of the light beam was controlled using a rotation stage (Hans Huber AG, Germany). A flow-cell consisting of a poly(dimethylsiloxane) gasket and a transparent glass bottom (volume approximately 25 μl) was attached to the sensor surface to contain liquid samples. The input and output ports of the flow-cell were connected to a peristaltic pump (Reglo, Ismatec, Switzerland) using rubber tubing (Tygon R3607, from Ismatec, Switzerland) to flow the liquid sample across the sensor surface (the flow rate of 50 $\mu\text{l min}^{-1}$ was used). The fluorescence light emitted by a dye at the sensor surface passed through the flow-cell, was collected using a lens, propagated through a bandpass filter (670FS10-25, L.O.T.-Oriel, Germany), and was projected into the input of a photomultiplier (H6240-01, Hamamatsu, Japan) that was connected to a counter (53131A, Agilent, USA). The optical setup and the data collection from the sensor was controlled using home-developed software.

Fig. 1 Optical setup of a sensor based on the angular spectroscopy of LRSPs for the detection of biomolecular binding using the measurement of refractive index variations and using the LRSP-enhanced fluorescence spectroscopy



Modification of the sensor surface for label-free and fluorescence-based measurements

To characterize the performance of the LRSP-based sensor, we monitored the binding of a labeled protein to the sensor surface. The binding of a labeled protein was observed at different distances from the gold sensor surface by using two strategies: a layer-by-layer adsorptive protocol and a fluoropolymer buffer layer were employed to reach the distances below 30 nm and above 30 nm, respectively.

For the layer-by-layer deposition, we firstly modified the gold surface with a mixed thiol self-assembled monolayer (SAM) [11]. The freshly evaporated gold was incubated overnight in the 9:1 mixture of 11-mercaptoundecan-1-ol and 11-mercapto-(8-biotinamido-4,7,dioxyaethyl)-undecanoyl-amid (total concentration 0.5 mM in ethanol), successively washed with ethanol and deionized water, dried with a stream of nitrogen, and loaded into the sensor. After, successive in situ immobilization of labeled streptavidin, biotinylated immunoglobulin, and labeled streptavidin layers to the gold surface was performed by bioaffinity binding from sequentially injected solutions containing respective analytes. The streptavidin with covalently attached Alexa Fluor 647 labels (AFSA, Molecular Probes, USA) was dissolved in phosphate buffer saline (PBS) at a concentration of $13.3 \mu\text{g ml}^{-1}$ and biotinylated goat antirabbit immuno-

globulin (IgG-biotin, Molecular Probes, USA, 2–8 biotin groups per molecule) was dissolved in PBS at a concentration of $10 \mu\text{g ml}^{-1}$. Each solution was flowed across the sensor surface for 10 min followed by a 5-min rinse of the surface with PBS. The saturation of protein binding to its bioaffinity partner on the surface was typically observed within 5 min. The thickness of the mixed thiol SAM was reported to be approximately 1 nm [11]. The thickness of AFSA and IgG-biotin layers were assumed to be of 6 and 18 nm, respectively, based on the data presented in the literature [12, 13]. By using these thicknesses, we estimated the average distance between the gold surface and Alexa Fluor 647 within the first AFSA layer as 4 nm. Because we observed a significantly lower surface coverage of AFSA and IgG-biotin compared to a close-packed monolayer, we assumed that binding of the second layer of AFSA has occurred inside the IgG-biotin layer. Therefore, we estimated the average distance between the gold surface and Alexa Fluor 647 located in the second AFSA layer to be roughly 19 nm.

To attach the AFSA to distances up to 500 nm from the gold surface, we spin-coated a Cytop spacer layer and a polystyrene (PS) layer onto the gold surface. The Cytop spacer layer was used because the refractive index of this fluoropolymer is very close to that of water and thus it does not perturb the propagation of LRSPs. The PS layer

(thickness of 12 nm) was prepared on its top as it is known to provide a surface to which efficient physisorption of proteins occurs. Before coating with the PS layer, the surface of the Cytop layer was etched a few angstroms deep with FluoroEtch (Acton Technologies, Ireland) to increase its surface energy. The immobilization of AFSA on top of the PS surface was performed in situ from the AFSA solution (dissolved in PBS at the concentration of $13.3 \mu\text{g ml}^{-1}$) flowed across the sensor surface for 10 min (the saturation of AFSA binding was typically observed after 5 min of incubation). After binding of AFSA, the surface was rinsed with PBS for 5 min.

Results and discussion

Characteristics of the thin gold films

For the excitation of LRSPs, we used gold films with thicknesses d_{Au} ranging from 15 to 30 nm deposited onto the Teflon AF and Cytop buffer layers. For the excitation of SPs, we used a 50-nm thick gold film deposited directly onto the BK7 glass. Firstly, we characterized the prepared gold films using an atomic force microscope. As illustrated in Fig. 2, when decreasing the thickness of the gold film, an increase of the roughness can be observed owing to the formation of gold islands. The root mean square roughness of gold films with the thicknesses of $d_{\text{Au}}=30, 22.5,$ and 15.8 nm deposited onto the Teflon AF was $\sigma=2.5, 3.7,$ and 3.9 nm , respectively. Gold films deposited onto the Cytop buffer layer exhibited lower roughness ($\sigma=3.7$ and 2 nm for $d_{\text{Au}}=22.5 \text{ nm}$ and Teflon AF and Cytop buffer layers,

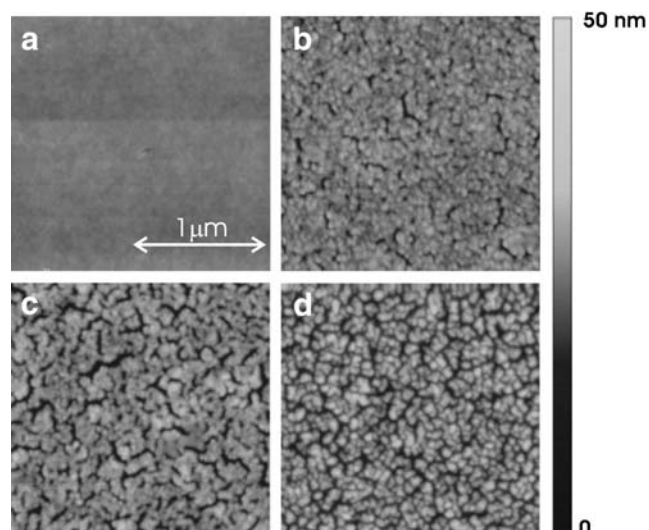
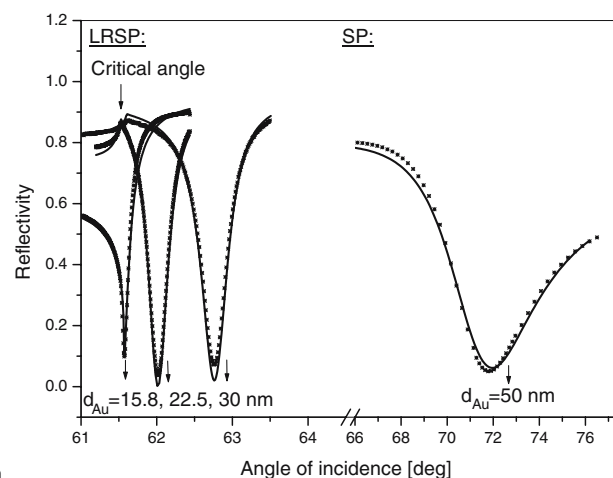
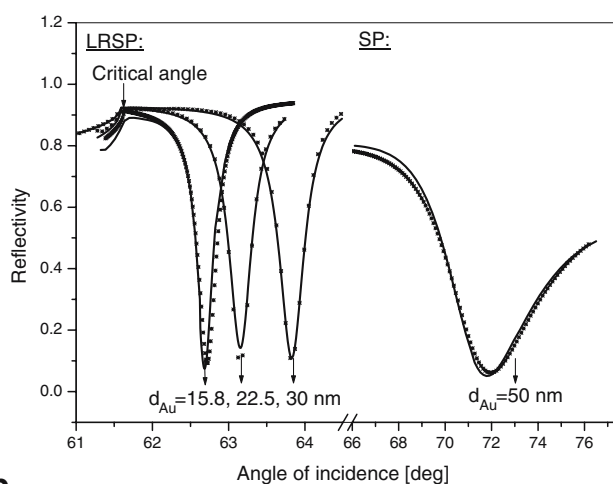


Fig. 2 Atomic force microscope characterization of **a** the surface of Teflon AF and of gold films deposited on its top with the thicknesses of **b** $d_{\text{Au}}=30 \text{ nm}$, **c** $d_{\text{Au}}=22.5 \text{ nm}$, and **d** $d_{\text{Au}}=15 \text{ nm}$



a



b

Fig. 3 Transverse-magnetic (TM) reflectivity spectra with a resonance dip as a result of the excitation of LRSPs on a gold film with thicknesses of $d_{\text{Au}}=15.8, 20,$ and 30 nm deposited on **a** Teflon AF buffer layer (thickness=603, 645, and 645 nm, respectively) and **b** Cytop (thickness=1,013, 895, and 695 nm, respectively). Surface brought in contact with water. Angle of incidence of a light beam (wavelength of $\lambda=632.8 \text{ nm}$) taken in BK7 glass. Asterisks represent the experiment, and solid lines represent the fitted theoretical function. For the comparison, angular spectrum for the excitation of SPs on the top of 50 nm thick gold film is shown

respectively). The roughness of the gold film with the thickness of 50 nm deposited on BK7 glass was $\sigma=0.82 \text{ nm}$, and the roughness of bare Teflon AF and Cytop layers was $\sigma=0.55$ and 0.50 nm , respectively.

To determine the impact of roughness to the optical properties of the gold films, we measured a series of angular reflectivity spectra for the excitation of LRSPs on these films and compared them to simulations based on the Fresnel theory, see Fig. 3. In these simulations, we assumed a homogenous gold film with an effective (complex) refractive index n_{Au} and a thickness d_{Au} . Before the

theoretical analysis, the thickness of the gold films d_{Au} and of the buffer layers were measured using a quartz crystal and a surface profiler, respectively. The refractive index of the Teflon AF and Cytop buffer layers were used as stated previously. By fitting the experiment, we determined the real and imaginary parts of the refractive index of gold films prepared on the Teflon and Cytop buffer layers. The obtained results presented in Fig. 4 reveal that the refractive index n_{Au} is not changing significantly for $d_{Au} > 25$ nm. For thicknesses $d_{Au} < 25$ nm, the real part of the refractive index $Re\{n_{Au}\}$ increases and the imaginary part $Im\{n_{Au}\}$ decreases when decreasing the thickness d_{Au} . Probably because of its lower roughness, the gold film deposited on the Cytop buffer layer exhibits a lower real part of the refractive index $Re\{n_{Au}\}$ comparing to that on Teflon AF. For each fluoropolymer buffer layer, we fitted the deter-

mined dependence of $Re\{n_{Au}\}$ and $Im\{n_{Au}\}$ on d_{Au} with an exponential function and used it in further simulations.

Characteristics of LRSPs

As shown in Fig. 3, the excitation of LRSPs manifests itself as a narrow dip in the angular reflectivity spectrum. Upon decreasing the thickness of the gold film, the resonant dip is shifted toward lower angles of incidence and its width is decreased. By comparing the reflectivity curves for Teflon AF and Cytop buffer layers presented in Fig. 3a and b, respectively, one can observe that resonances for the Teflon AF buffer layer are located at lower angles of incidence with respect to those for the Cytop buffer layer. The reason for this difference is the lower refractive index of Teflon AF ($n_{AF}=1.308$) compared to that of Cytop (refractive index $n_{Cytop}=1.340$). The resonance dips for the excitation of LRSPs are observed closer to the critical angle and they exhibit more than an order of magnitude lower width than that for conventional SPs (e.g., the full width in the half minimum of $\Delta\theta_{FWHM}=0.12^\circ$ was observed for LRSPs excited on the 15.8 nm thick gold film on the Teflon AF buffer layer compared to 5° for the excitation of conventional SPs). As the excitation of LRSPs occurs closer to the critical angle, their penetration depth L_p into the water medium is higher than that for SP. As seen in simulations presented in Fig. 5a, the penetration depth L_p (distance at which the field amplitude decreases by a factor of $1/e$) is significantly larger for the LRSP guided along the gold film on the Teflon AF buffer layer ($L_p=5,000$ nm for $d_{Au}=15$ nm) compared to that for the LRSP on the Cytop buffer layer ($L_p=550$ nm for $d_{Au}=15$ nm) and for the SP ($L_p=190$ nm). As the refractive index of Teflon AF is lower than that of water $n_{AF} < n_{water}$, the penetration depth of LRSP guided on the top of this buffer layer is diverging when approaching the cut-off thickness of the gold film (smallest thickness for which LRSP exists on this refractive index asymmetric structure). The refractive index of Cytop is higher than that of water $n_{Cytop} > n_{water}$, and thus only LRSPs with a L_p below a certain value can be excited using this buffer layer:

$$L_p = \left(\frac{2\pi}{\lambda}\right) \sqrt{n_{Cytop}^2 - n_{water}^2} \tag{1}$$

To determine the enhancement of the electromagnetic field caused by the excitation of LRSPs, we calculated the profile of the magnetic intensity across the layer structure for the thicknesses of the gold film ranging from $d_{Au}=15$ to 30 nm and for the Teflon AF and Cytop buffer layers. For each d_{Au} , we determined the thickness of a buffer layer that gained maximum coupling to LRSPs, see Fig. 5b. The

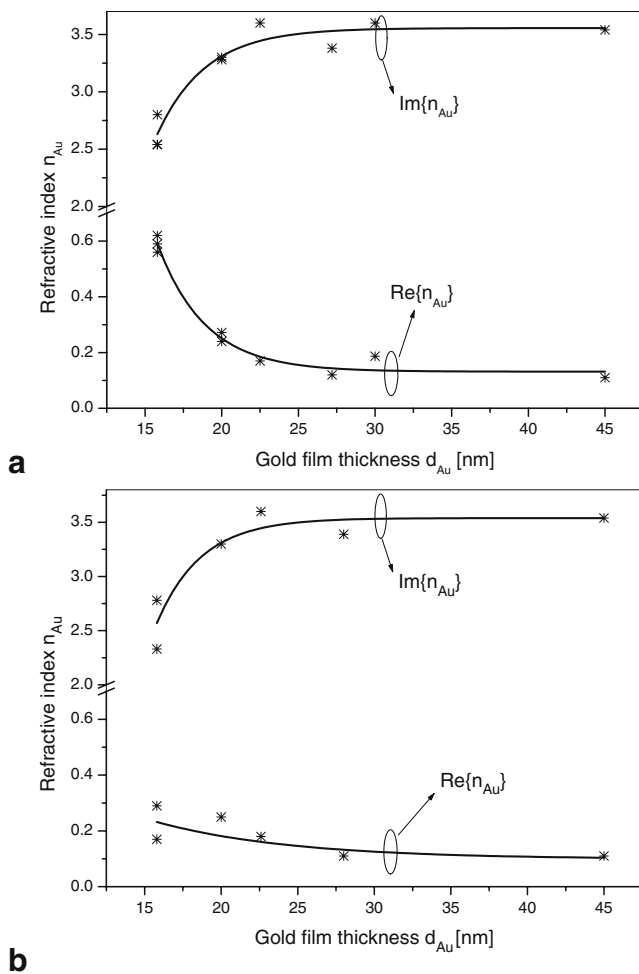


Fig. 4 The dependence of the real and imaginary parts of the refractive index of gold $Re\{n_{Au}\}$ and $Im\{n_{Au}\}$ on the thickness d_{Au} for a gold film deposited on **a** Teflon AF and **b** Cytop buffer layers; the wavelength of $\lambda=632.8$ nm

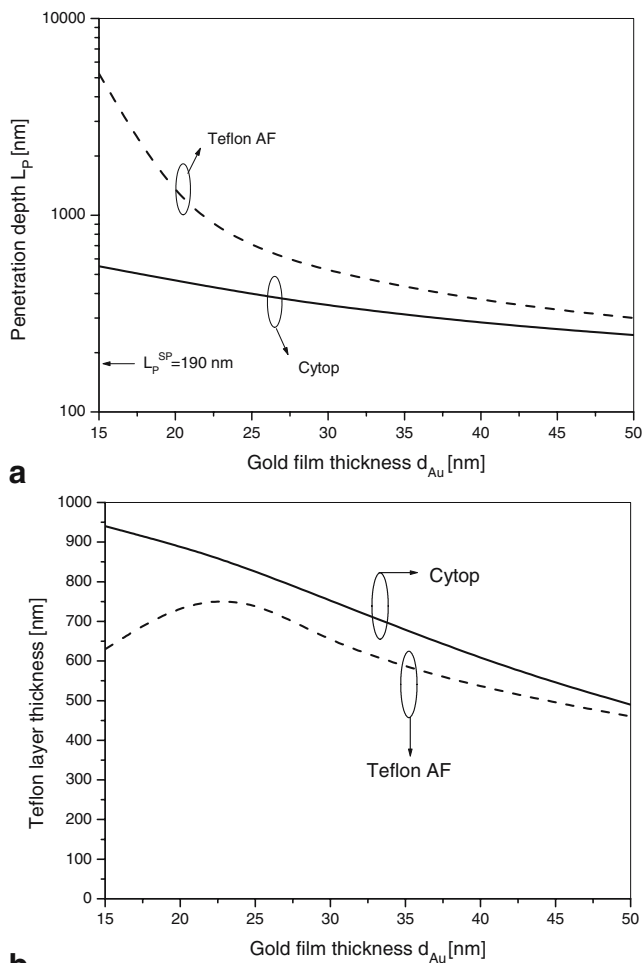


Fig. 5 **a** Penetration depth of LRSP L_p into the water medium for a gold film with a thickness in the range $d_{Au}=15\text{--}50$ nm, and Teflon AF (dashed line) and Cytop (solid line) buffer layers. **b** Optimum thickness of Teflon AF (dashed line) and Cytop buffer (solid line) layers providing the full coupling to LRSPs on gold films with the thickness in the range $d_{Au}=15\text{--}50$ nm

profiles of magnetic intensity were calculated for the angles of incidence close to the resonance at which the highest field enhancement occurs. Figure 6a and b shows the obtained results for layer structures with the Teflon AF and Cytop buffer layers, respectively, and for the gold film thicknesses of $d_{Au}=15, 20,$ and 30 nm. They reveal that the maximum field intensity of LRSPs occurs at the inner surface of gold film for the Teflon AF buffer layer and at the outer surface of gold film for the Cytop buffer layer. With respect to the excitation of SPs, higher enhancement of the electromagnetic field intensity is observed at the outer surface of the gold film (interface between the gold film and water) for the excitation of LRSPs. The highest enhancements of 42 and 59 are predicted for LRSPs guided on the 20-nm thick gold film and Teflon AF and Cytop buffer layers, respectively, compared to 16.5 for conven-

tional SPs. For $d_{Au}<20$ nm, the field enhancement is decreased as losses in gold film increase significantly (see Fig. 4).

LRSP-based sensor utilizing measurements of refractive index variations

In this section, we characterize the LRSP-based sensor operated in the refractometric mode and compare its performance to that of conventional SPR sensor. The main characteristic of a sensor is its resolution which defines the smallest change in a measured quantity δc that produces a detectable change in the sensor output δY . In SPR sensors relying on the measurement of refractive index variations, δY is typically a change in the resonant wavelength $\delta\lambda_{res}$ (wavelength spectroscopy of SPs) or angle of incidence

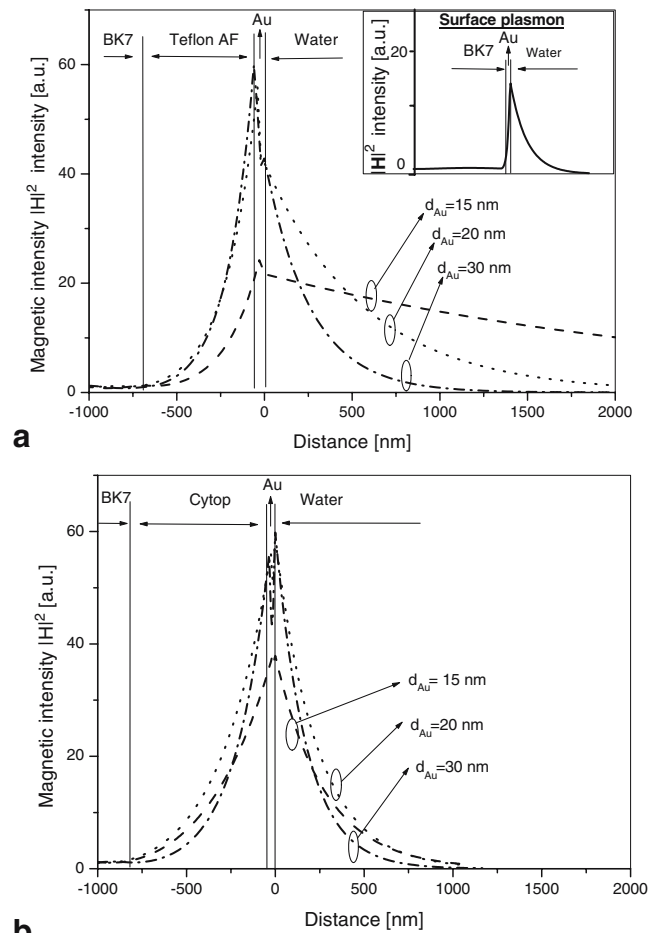


Fig. 6 Simulations of magnetic intensity field profile for LRSPs excited on a gold film with the thicknesses of $d_{Au}=15, 20,$ and 30 nm on the top of **a** Teflon AF and **b** Cytop buffer layers. LRSPs are excited with an optical wave propagating in a BK7 glass incident at the layer structure under the resonant angle of incidence. The magnetic intensity $|H|^2$ of the wave incident wave from BK7 glass is normalized to 1. The dependence of the field distribution of the conventional SP is shown for the comparison

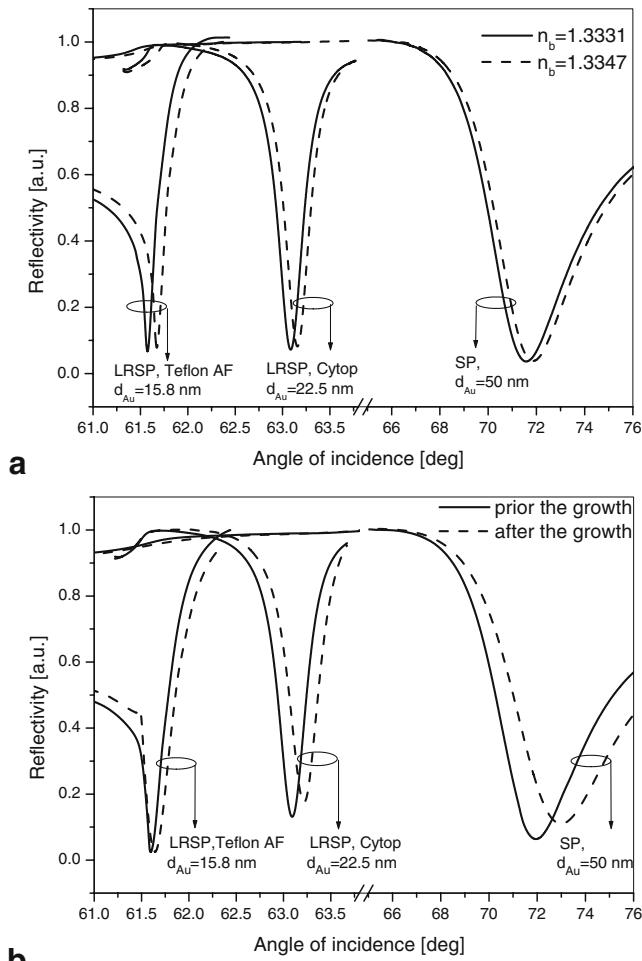


Fig. 7 Measured shifts in the reflectivity dip as a result of the excitation of LRSPs induced by **a** a bulk refractive index change $\delta n_B = 1.6 \times 10^{-3}$ RIU and **b** by a growth of a protein multilayer on the sensor surface. Gold layer thickness of $d_{Au} = 22.5$ nm (Cytop buffer layer) and $d_{Au} = 15.8$ nm (Teflon AF) buffer layer. Shifts of conventional SPR dips as a result of identical refractive index changes are shown for the comparison

$\delta\theta_{res}$ (angular spectroscopy of SPs). In general, a change in the sensor output δY caused by a change in the measured quantity δc can be expressed as:

$$\delta Y = \frac{dY}{dn} \frac{dn}{dc} \delta c = S_{RI} \frac{dn}{dc} \delta c, \tag{2}$$

where dn is the refractive index change induced by the measured quantity and S_{RI} is the refractive index sensitivity. For most commonly used modulations of SPR, the resolution of a SPR sensor is inversely proportional to:

$$\chi = \frac{S_{RI}}{w}, \tag{3}$$

where w is the width of the SPR dip. The parameter χ depends only weakly on the choice of the modulation of SPR [14]. Therefore, without the loss in generality, we

further analyze the improvement in resolution of the LRSP-based sensor by using the χ parameter and the angular spectroscopy (δY states for a change in the resonant angle of incidence $\delta\theta_{res}$ and w is the angular width of the resonance dip $\Delta\theta_{FWHM}$).

Firstly, we analyze the χ parameter for bulk refractive index changes δn_B . In the experiments, we used structures with the gold film thicknesses of $d_{Au} = 15.8$ and 22.5 nm and with the Cytop and Teflon AF buffer layers. For each d_{Au} , the thickness of the Cytop and Teflon AF buffer layers providing maximum coupling to LRSPs was used (see Fig. 5b). From such structures, we measured resonance reflectivity spectra for the excitation of LRSPs if solutions with bulk refractive index of $n_{B1} = 1.3331$ (water) and $n_{B2} = 1.3347$ RIU (1.6% ethylene glycol in water) were flowed across the sensor surface. As seen in Fig. 7a for two

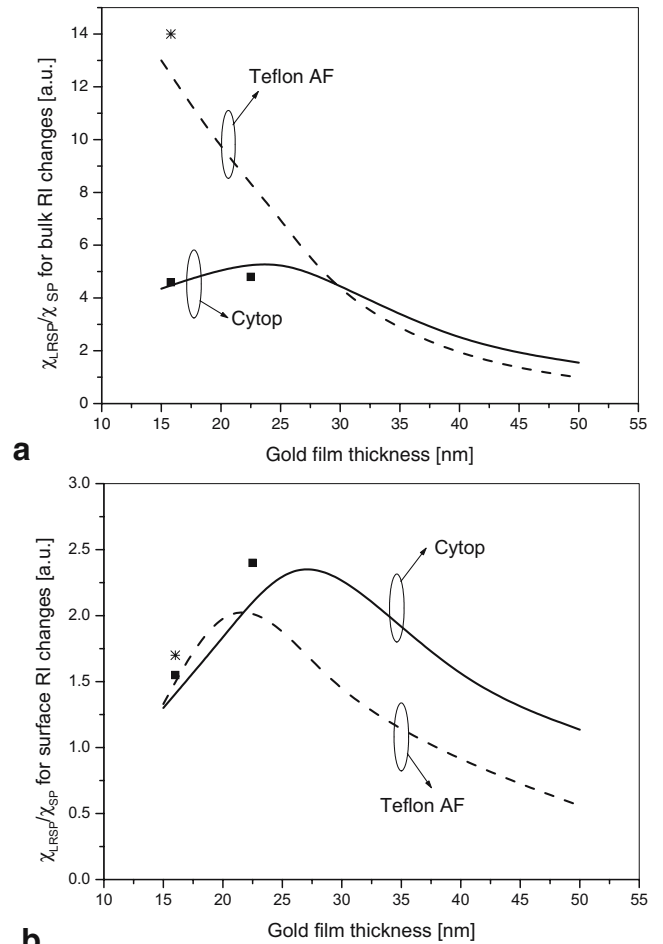


Fig. 8 The dependence of χ parameter for the observation of refractive index changes in **a** whole evanescent field of LRSP and **b** at the close proximity to the metal surface on the gold film thickness. Results obtained from experiments (asterisks and squares represent the results for the Teflon AF and Cytop buffer layers, respectively) are compared to those from simulations (dashed line and solid line represent the results for the Teflon AF and Cytop buffer layers, respectively). The parameter χ for LRSP-based sensor is normalized with the one for a conventional SPR sensor

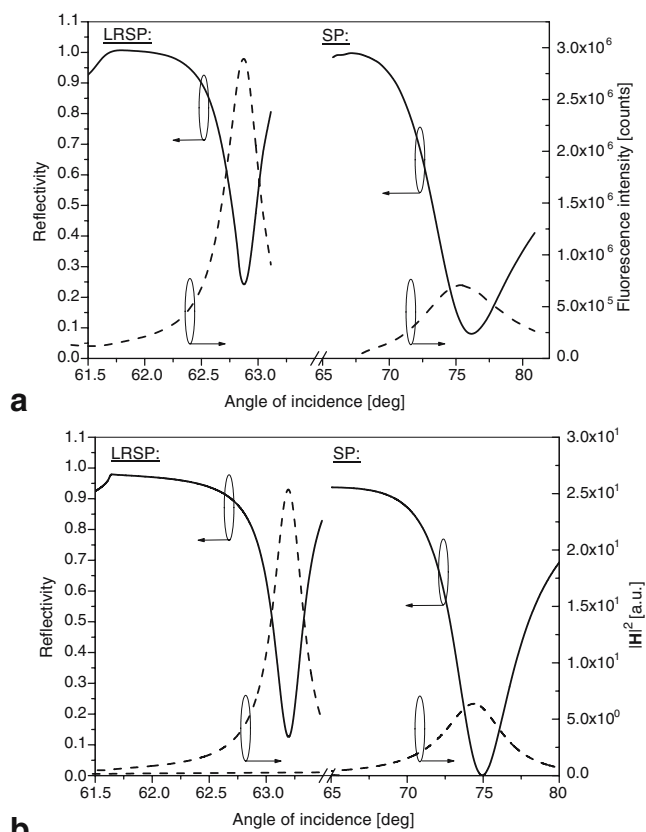


Fig. 9 **a** LRSP angular spectra of the reflectivity and fluorescence intensity measured for an AFSA layer deposited at the (average) distance of 42 nm from the sensor surface (LRSP excited on gold film with $d_{\text{Au}}=15.8$ nm on top of the Cytop buffer layer), **b** simulations of the reflectivity and magnetic field intensity enhancement for identical configurations as in **a**

structures supporting LRSPs (a gold film with $d_{\text{Au}}=15.8$ nm on the Teflon AF buffer layer and a gold film with $d_{\text{Au}}=22.5$ nm on the Cytop buffer layer) and for the excitation of SPs, the increase in the bulk refractive index n_B induces a shift of the resonance dips toward higher angles of incidence. From the observed shifts $\delta\theta_{\text{res}}$ and resonance widths $\Delta\theta_{\text{FWHM}}$, we determined the χ parameter for the excitation of LRSPs (χ_{LRSP}) and compared it with that for a conventional SPR sensor (χ_{SP}). Obtained results reveal that the highest improvement (factor of $\chi_{\text{LRSP}}/\chi_{\text{SP}}=14$) is achieved for the gold film with the thickness of $d_{\text{Au}}=15.8$ nm on the Teflon AF buffer layer. The comparison of measured ratios $\chi_{\text{LRSP}}/\chi_{\text{SP}}$ with simulations presented in Fig. 8a reveals very good agreement. These results show that the LRSP-based sensor and the Teflon AF buffer layer outperforms the one with the Cytop buffer layer as LRSPs guided in such structure carry the highest portion of electromagnetic field in the sensed medium (see Fig. 6a) and exhibit the lowest resonance width (see Fig. 3a).

Next, using the same layer structures, we measured the angular shifts $\delta\theta_{\text{res}}$ caused by a surface refractive index

change δn_S produced by the successive growth of protein layers of AFSA, IgG-biotin and AFSA on the gold surface (procedure described above). The measured resonance reflectivity before and after the deposition of the protein multilayer are shown in Fig. 7b for two structures supporting LRSPs (a gold film $d_{\text{Au}}=15.8$ nm on the Teflon AF buffer layer and a gold film with $d_{\text{Au}}=22.5$ nm on the Cytop buffer layer) and for conventional SPR. Similarly, as in the previous section, we determined the ratio $\chi_{\text{LRSP}}/\chi_{\text{SP}}$ for each structure and compared it with simulations, see Fig. 8b. These results show very good agreement and they reveal that the highest improvement in the sensor resolution ($\chi_{\text{LRSP}}/\chi_{\text{SP}}=2.4$) can be achieved for LRSPs guided along the gold film with $d_{\text{Au}}=22.5$ nm on the Cytop buffer layer. For the measurement of surface refractive index variations δn_S , the layer structure with the Cytop buffer layer offers the higher resolution compared to that with Teflon AF because it supports LRSPs with the higher intensity of electromagnetic field at the interface between the gold film and an aqueous sample (compare Fig. 6a and b). The decrease in the $\chi_{\text{LRSP}}/\chi_{\text{SP}}$ for the gold films with thickness $d_{\text{Au}}<25$ nm is observed because of the increased damping in these films (see Fig. 4).

Sensor based on LRSP-enhanced fluorescence spectroscopy

In this study, we measured the fluorescence intensity of the dye Alexa-Fluor 640 deposited at different distances from the sensor surface on which LRSPs or conventional SPs were excited. The distance between the dye and the sensor surface was controlled by layer-by-layer deposition (distances <30 nm) and by means of fluoropolymer spacer layer (distances >30 nm) as described above. This study was

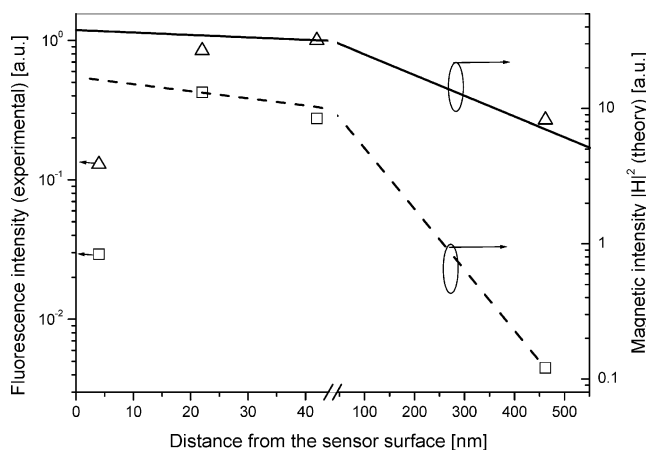


Fig. 10 Measured fluorescence intensity of light emitted by Alexa Fluor 670 dye at the distance between 4 and 460 nm excited with SPs (squares) and LRSPs (triangles) guided along the gold film with the thickness of $d_{\text{Au}}=15.8$ nm on top of the Cytop buffer layer. For the comparison, theoretical dependence of the maximum magnetic intensity field enhancement on the distance from the gold surface for the excitation of SP (dashed line) and the LRSP (solid line) is shown

performed for the excitation of dyes with LRSPs guided in the structures with the Cytop buffer layer and gold film thickness of $d_{\text{Au}}=15.8$ nm and 22.5 nm. The fluorescence intensity was normalized with the intensity of a light beam coupled to (LR)SPs and compensated for the background fluorescence signal measured before the deposition of the dye. In addition, the differences in the fluorescent intensity because of the variability of surface coverage of the dye attached by the layer-by-layer deposition and by the physisorption on the top of the fluoropolymer spacer layer were taken to account.

We measured the angular fluorescence and reflectivity spectra for dyes bound at distances of 4, 19, 42, and 460 nm from the surface of the layer structures supporting LRSPs and conventional SPs. In Fig. 9a, we show the comparison of typical reflectivity and fluorescence spectra for a dye excited by LRSPs and conventional SPs. These results show that for the excitation by LRSPs, the fluorescence intensity is detected within a narrower band of angles of incidence and exhibits higher peak intensity than for the excitation by conventional SPs. In general, the comparison of experimental and theoretical spectra revealed very good agreement in terms of angular position and width of the resonance reflectivity dips and the fluorescence peaks (see Fig. 9b). Moreover, the experimental ratio of the peak fluorescence intensity for the excitation of LRSPs and SPs was in a good agreement with the calculated field enhancement ratio.

In Fig. 10, we present the dependence of the peak fluorescence intensity on the distance of the dye from the sensor surface when excited by LRSP (for $d_{\text{Au}}=15.8$ nm and the Cytop buffer layer) and conventional SPs. These results reveal that the fluorescence peak intensity reaches its maximum if dyes are placed between 20 and 40 nm from the sensor surface. For the lowest distance of 4 nm, we observed a drop in the peak fluorescence intensity caused by the nonradiative decay of a dye induced by the presence of the metal medium [15]. At distances larger than 40 nm, the fluorescence intensity decays exponentially and follows the trend of the electromagnetic field enhancement obtained from simulations. The maximum peak intensities of the fluorescence were observed for LRSPs guided along the 15.8 nm thick gold film. With respect to the excitation of conventional SPs, the fluorescence intensity enhancement of 4.4, 2.0, 4.1, and 60 was measured at the distances 4, 19, 42, and 460 nm from the sensor surface, respectively. For the excitation of dyes distributed within the whole evanescent field of LRSP and SP, the overall enhancement in the collected fluorescence intensity can be assumed as the product of the enhancement at the proximity to the sensor surface (4.4 measured at the distance 4 nm) and the ratio of penetration depths (for LRSP with $d_{\text{Au}}=15.8$ nm and conventional SP this ratio is equal to 2.9). By this

means, we can estimate that more than 12-fold increase in the fluorescence intensity can be achieved by taking advantage of the higher enhancement and more extended field of LRSP when compared with conventional SPs.

Conclusions

In conclusion, we demonstrated that LRSPs enables advancing current SPR biosensors based on label-free detection of RI changes and on SP-enhanced fluorescence spectroscopy. Through the careful design of a layer structure supporting LRSPs, we achieved a 2.5- and 14-fold improvement of the resolution in the measurement of RI changes occurring at the surface and in the bulk medium, respectively, compared to conventional SPR sensors. Moreover, with respect to conventional SPR, a 4.4- and 12-fold enhancement in measured fluorescence intensity was observed if labeled molecules were bound at the surface and distributed within the whole evanescent field of LRSP, respectively. Future research will be aimed at improving the quality of ultrathin gold films, which exhibited increased roughness, and at combining of presented LRSP-based sensor with three-dimensional binding matrices. Using such matrices (e.g., dextran brushes or hydrogels), the biomolecular binding events can be probed with the whole field of LRSPs. This configuration is expected to provide over an order of magnitude higher resolution in both label-free and fluorescence spectroscopy-based detection by taking advantage of lower damping and higher penetration depth of LRSPs.

Acknowledgements Partial support for this work was provided by the Deutsche Forschungsgemeinschaft (KN 224/18-1, Schwerpunktprogramm “Intelligente Hydrogele”, JPP 1259) and by the EU through FP6-2005-FOOD-036300 (“TRACEPACK”).

References

1. Rather H (1983) Surface plasmons on smooth and rough surfaces and on gratings. Springer, Berlin Heidelberg New York
2. Homola J, Yee SS, Gauglitz G (1999) Surface plasmon resonance sensors: review. *Sens Actuators, B, Chem* 54:3–15
3. Liebermann T, Knoll W (2000) Surface-plasmon field-enhanced fluorescence spectroscopy. *Colloids Surf, A Physicochem Eng Asp* 171:115–130
4. Sarid D (1981) Long-range surface-plasma waves on very thin metal-films. *Phys Rev Lett* 47:1927–1930
5. Craig AE, Olson GA, Sarid D (1983) Experimental observation of the long-range surface-plasmon polariton. *Opt Lett* 8:380–382
6. Matsubara K, Kawata S, Minami S (1990) Multilayer system for a high-precision surface-plasmon resonance sensor. *Opt Lett* 15:75–77
7. Nenninger GG, Tobiska P, Homola J, Yee SS (2001) Long-range surface plasmons for high-resolution surface plasmon resonance sensors. *Sensors and Actuators B-Chemical* 74:145–151

8. Slavik S, Homola J (2007) Ultrahigh resolution long range surface plasmon-based sensor. *Sens Actuators, B, Chem* 123:10–12
9. Wark AW, Lee HJ, Corn RM (2005) Long-range surface plasmon resonance imaging for bioaffinity sensors. *Anal Chem* 77:3904–3907
10. Kasry A, Knoll W (2006) Long range surface plasmon fluorescence spectroscopy. *Appl Phys Lett* 89:101106
11. Knoll W, Zizlsperger M, Liebermann T, Arnold S, Badia A, Liley M, Piscevic D, Schmitt FJ, Spinke J (2000) Streptavidin arrays as supramolecular architectures in surface-plasmon optical sensor formats. *Colloids Surf, A Physicochem Eng Asp* 161:115–137
12. Swann MJ, Peel LL, Carrington S, Freeman NJ (2004) Dual-polarization interferometry: an analytical technique to measure changes in protein structure in real time, to determine the stoichiometry of binding events, and to differentiate between specific and nonspecific interactions. *Anal Biochem* 329:190–198
13. Malmsten M (1994) Ellipsometry studies of protein layers adsorbed at hydrophobic surfaces. *J Colloid Interface Sci* 166:333–342
14. Homola J, Piliarik M (2006) SPR sensor instrumentation. In: Homola J (ed) *Surface plasmon resonance based sensors*. Springer, Berlin Heidelberg New York, pp 45–69
15. Vasilev K, Knoll W, Kreiter M (2004) Fluorescence intensities of chromophores in front of a thin metal film. *J Chem Phys* 120:3439–3445